Scientific Research Publishing

American Journal of Plant Sciences, 2026, 17(11), 1369-1394
https://www.scirp.org/journal/ajps
ISSN Online: 2158-2750
ISSN Print: 2158-2742

Changes in Land Cover and Land Use in the Aïr and Ténéré National Nature Reserve (RNNAT) in Niger

Adamou Hamadou Wankoye[1], Abdoulaye Abdou Siradji[2], Ali Ado[3*], Seghieri Josiane[4]

[1]Doctoral School of Peace, Security, Environment and Sustainable Development, University of Diffa, Diffa, Niger
[2]Faculty of Sciences and Technology, Abdou Moumouni University, Niamey, Niger
[3]National School of Engineering and Energy Sciences, University of Agadez, Agadez, Niger
[4]CIRAD, INRA, IRD, Montpellier SupAgro, University of Montpellier, Montpellier, France
Email: *aaliado@gmail.com

How to cite this paper: Wankoye, A.H., Siradji, A.A., Ado, A. and Josiane, S. (2026) Changes in Land Cover and Land Use in the Aïr and Ténéré National Nature Reserve (RNNAT) in Niger. *American Journal of Plant Sciences*, **17**, 1369-1394.
https://doi.org/10.4236/ajps.2026.1711083

Received: June 23, 2026
Accepted: November 24, 2026
Published: November 27, 2026

Copyright © 2026 by author(s) and Scientific Research Publishing Inc.
This work is licensed under the Creative Commons Attribution International License (CC BY 4.0).
http://creativecommons.org/licenses/by/4.0/

Open Access

Abstract

Forest areas are, on a global scale, one of the primary tools for preserving biodiversity and the services it provides to human societies. The objective of this study is to assess the dynamics of land use within the reserve. To this end, satellite images from the Landsat series (2000, 2005, 2015, and 2025) were downloaded from the United States Geological Survey (USGS) website (http://earthexplorer.usgs.gov/). Supervised classification was used to convert and analyze the information from the raster images into a thematic map. Consequently, the pixels in each image were classified using the maximum likelihood algorithm, which was applied to all images from 2000, 2005, 2015, and 2025. The spatial structure analysis revealed that five land-use units were identified (rock outcrops; riparian strips; steppe; Ténéré ergs; and guelta/mare) and five categories of spatial change over a 25-year period. These include fragmentation, dissection, aggregation, creation, and removal. It appears that between 2000 and 2005, the riparian strip, steppe, and Guelta/Mare classes experienced positive rates of change with respective values of 1.94, 0.19, and 0.84. However, the "Rock Outcrop" and "Ténéré Erg" classes experienced negative growth rates of −0.54 and −0.06, respectively. This decline was caused by droughts or human activities (large-scale gold panning, overgrazing, and unregulated occupation of irrigated plots) during the 2015-2025 period. Thus, it is urgent to take appropriate measures to reverse the current trend in the RNNAT.

Keywords

Dynamic, Riparian, Erg ef Ténéré, Steppe, Rack Guelta

1. Introduction

Forests are one of the most important tools worldwide for preserving biodiversity and the services it provides to human societies [1]. They are also key components of strategies to mitigate climate change [2]. Since the Industrial Revolution, changes in land cover and land use have accelerated due to agricultural expansion, urbanization, and increased exploitation of natural resources, contributing to global change [3]. Currently, the impacts of climate change are giving forests a renewed role as tools for adapting to climate change.

In Niger, as in many regions of West Africa and the Sahel, these protected areas are subject to numerous forms of rapidly increasing human pressure [4]. This is the case for the Aïr and Ténéré National Nature Reserve (RNNAT), designated on January 22, 1988, to preserve the exceptional biodiversity of this Saharan ecosystem, a fact reaffirmed by the international scientific community [4] and [5], Yet this reserve encompasses the bulk of Saharan biodiversity due to its ecosystem diversity [6], However, the reserve's ecosystems and their surrounding areas face intensive land use, characterized by the illegal expansion of irrigated crops; increasing pressure on timber resources to supply urban centers; gold mining, and intensive livestock farming [7]-[9]. According to [10], the environmental impacts of gold mining are enormous. Indeed, the land is stripped bare by prospecting, and the waste dumps around the mines release significant amounts of dust, degrading the vegetation cover and the already scarce pastoral resources—not to mention the increased demand for charcoal for cooking, which accelerates deforestation throughout the region. Furthermore, this region is the Saharan part of Niger, where rain falls only for a short period in July and August [11].

This situation raises concerns among managers and impacts the vital subsistence needs of local populations. Therefore, it is important to ask how land use shapes the forest cover of the RNNAT and what solutions exist for restoration and sustainable management?

To answer this question, our analysis will focus on the following main areas: first, we will assess the current state of land-use dynamics within the reserve; second, we will evaluate the environmental and socioeconomic consequences of this phenomenon; and finally, we will propose participatory planning and management strategies to reconcile local development with the protection of biodiver.

2. Materials and Methods

2.1. Study Area

This study was conducted in the Aïr and Ténéré National Nature Reserve (RNNAT). The reserve covers an area of 7,736,000 hectares (**Figure 1**); its central section (1,280,500 ha) is designated as a strict nature reserve (an Addax sanctuary), and the entire area is located in the Agadez department of northern Niger, between 17˚12' and 20˚30' North latitude and 8˚06' and 10˚57' East longitude. Established by Decree No. 88-019/PCMS/MAG/E on January 22, 1988, the reserve extends between the Aïr Mountains (with peaks reaching 2200 meters) and the Ténéré

Desert. The RNNAT was designated a World Heritage Site in 1991 and subsequently a Biosphere Reserve in 1997. It falls under IUCN categories II and I [12]. This classification is justified by the exceptional quality of the biodiversity found within this Saharan ecosystem [13]. It exhibits a markedly asymmetrical morphology. Its western section consists of a peneplain with an average elevation of 700 to 800 meters, deeply incised by a westward-flowing drainage network. According to the Köppen-Geiger classification, the climate of the Agadez region is desert-like; more specifically, it ranges from arid to hyper-arid. The annual cycle is characterized by a long dry season (October-May) and a short rainy season (July-September) [13]. Mean annual temperatures of 28˚C and average annual precipitation of less than 150 mm are recorded. Vegetation distribution is irregular; the reserve's plant landscape comprises two main types: the "contracted" vegetation found on the terrain of the Aïr Massif, and the vegetation of the vast sandy expanses of the Ténéré—which is either ephemeral or virtually [13] [14].

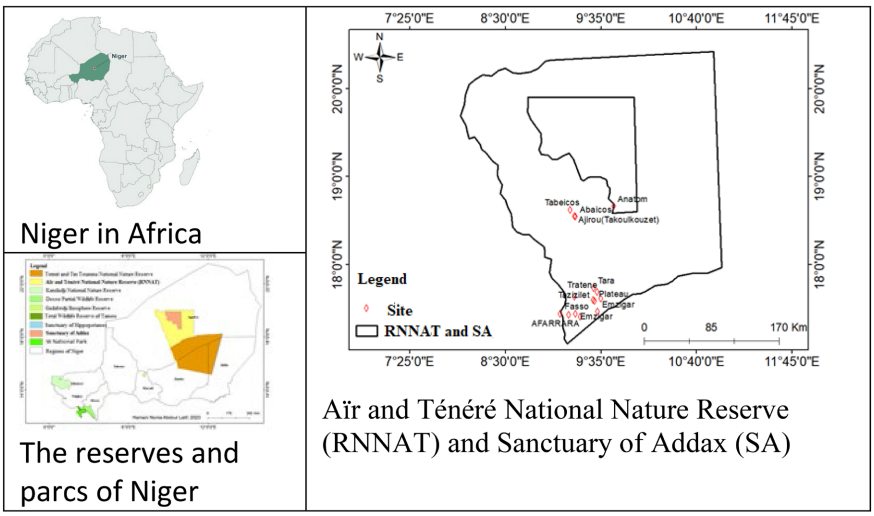


Figure 1. Study area.

2.2. Data Acquisition

A single data source was used to determine the dynamics of land cover in the RNNAT. Specifically, this included satellite imagery from the Landsat series for the years 2000, 2005, 2015, and 2025.

Furthermore, the images were downloaded from the United States Geological Survey (USGS) website (http://earthexplorer.usgs.gov/), which shed light on landscape land-use dynamics at four specific dates: 2000; 2005; 2015; and 2025—covering a total period of 25 years. These reference years were chosen to cover a period of five (5) to ten (10) years during which a change can be observed between two (2) dates [15]. Furthermore, the choice of the first date—2000—is justified because, following a thorough review of the imagery, it was only as of this date that the entire area of RNNAT was covered by 8 satellite images and 24 satellite strips.

It should be noted that the scenes were selected based on their preprocessing quality. Indeed, the scenes were downloaded between the end of the winter season

and the beginning of the dry season. During this time of year, there is a significant reduction in cloud cover [16]. This helps avoid comparing images from different seasons, which could lead to inaccurate results [17]. hapefiles comprising a georeferenced digital layer of Niger—including road networks, administrative units, village locations, and certain water sources—were also used. GPS data collected in the field were also used to provide additional information [18] (**Table 1**).

Table 1. Characteristics of the downloaded Landsat scenes (http://earthexplorer.usgs.gov/).

Satellites	Sensors	Rom and path	Acquisition Date Range	Spatial Resolution	Bands
Scènes des images 2025					
Landsat 8	OLI + TIRS	188-046 188-047 188048	20251011_20251117_02_T1	**30 m**	6-5-4
Landsat 9	OLI-2 + TIRES-2	189-046	20251026_20251113_02_T1	**30 m**	6-5-4
		189-047	20251026_20251113_02_T1		6-5-4
		189-048			6-5-4
Landsat 8	OLI + TIRS	190-046	_20251025_20251121_02_T1	**30 m**	6-5-4
Landsat 9	OLI-2 + TIRES-2	190-047	_20251017_20251027_02_T1		6-5-4
Scènes des images 2015					
Landsat 8	OLI + TIRS	188046 188047	20151117_20200908_02_T1	**30 m**	6-5-4
		188048	20151016_20200908_02_T1		6-5-4
		189046 189047 189048	20151007_20200908_02_T1	**30 m**	6-5-4
		190046 190047	20151014_20200908_02_T1	**30 m**	6-5-4
Scènes des images 2015					
Landsat 7	TM	188046 188047 188048	20051028_20200914_02_T1	**30 m**	5-4-3
		189046 189047 189048	20051019_20200914_02_T1	**30 m**	5-4-3
		190046	20051026_20200914_02_T1	**30 m**	5-4-3
		190047	20051111_20200914_02_T1		5-4-3
Scènes des images 2000					
Landsat 7	TM	188046	20001201_20200917_02_T1	**30 m**	5-4-3
		188047	20000320_20200918_02_T1		5-4-3
		188048	20000507_20200918_02_T1		5-4-3
		189046	20001106_20200917_02_T1		5-4-3
		189047 189048	20001021_20200918_02_T1		5-4-3
		190046 190047	20001028_20200918_02_T1	**30 m**	5-4-3

Continued

Satellites	Sensors	Acquisition Date Range	Spatial Resolution	Bands
Landsat 8/9	OLI + TIRS/OLI-2 + TIRES-2	11/10/2025 à 26/10/2025	30 m	6-5-4
Landsat 8	OLI + TIRS	07/10/2016 à 17/11/2015		
Landsat 7	TM	09/10/2005 à 11/11/2005	30 m	5-4-3
	TM	20/03/2000 à 01/12/2000		

2.3. Field Visit

During this study, a reconnaissance field visit was conducted within the Aïr and Ténéré National Nature Reserve (RNNAT) and its surrounding areas in Agadez, Niger. To better describe the sites, the three municipalities (Tamia, Iferouāne, and Tabelot) that are part of the RNNAT were sampled. At each site, the following information was collected: vegetation type; the most and least dominant plant species; and the geomorphology of the terrain (plateau, slope, mid-slope, lowland).

2.4. Image Preprocessing

This step, which preceded the actual processing, involved applying radiometric and geometric corrections to the 5-4-3 bands from 2000 and filling in gaps in the 5-4-3 bands of Landsat 7TM data from 2005 for all scenes covering the reserve. To do this, QGIS software was used for the preprocessing of the gaps. This involved correcting the gaps observed in the 2005 Landsat 7 images. To do this, spectral bands 5-4-3 were imported into the QGIS interface as a raster layer using the "Add Raster Layer" tool.

Each band was then processed individually. After selecting the relevant band, the "Fill NoData" tool—available in QGIS's raster analysis tools—was used to fill in areas with missing values. After configuring the tool's settings, the process was started by clicking "Run." Finally, each resulting raster was renamed according to its corresponding band number. The same procedure was repeated for each of the spectral bands in question.

In addition, a radiometric correction was applied to the Landsat 7TM images from 2000. This involved removing atmospheric artifacts so that the pixels would be clear and classifiable. Comparability among the different satellite images was ensured by applying this entire preprocessing sequence, which aimed to standardize their geometric, radiometric, and spatial characteristics, as well as their identical spatial resolutions (30 m).

2.5. Satellite Image Processing

Several steps were followed during the processing of the satellite images.

Color Composition

Color composition involves creating color images by taking into account the spectral signature of objects [19]. Thus, two types of color composition can be distinguished: true-color composition and false-color composition (reference).

This approach has the advantage of distinguishing between different ground objects in the area of interest, particularly vegetation, which has high reflectance [20].

For this study, false-color composition was chosen for all bands. Thus, bands 6-5-4 of the Landsat 8 and 9 images were assigned to the SWIR 1, near-infrared, and red channels for the years 2015 and 2025. Specifically, band 6 (SWIR 1) is assigned to the red channel, band 5 (near-infrared) to the green channel, and band 4 (red) to the blue channel. Furthermore, bands 5, 4, and 3 from the 2000 and 2005 Landsat 7TM images are used in the various channels as follows: band 5 for red, band 4 for green, and band 3 for blue.

Mosaicking

Mosaicking is a necessary step following the processing of satellite images. It involves assembling multiple scenes covering the entire study area into a single, homogeneous image. Given the size of RNNAT, eight scenes with different paths and rows are required to cover all of its areas (**Figure 2**).

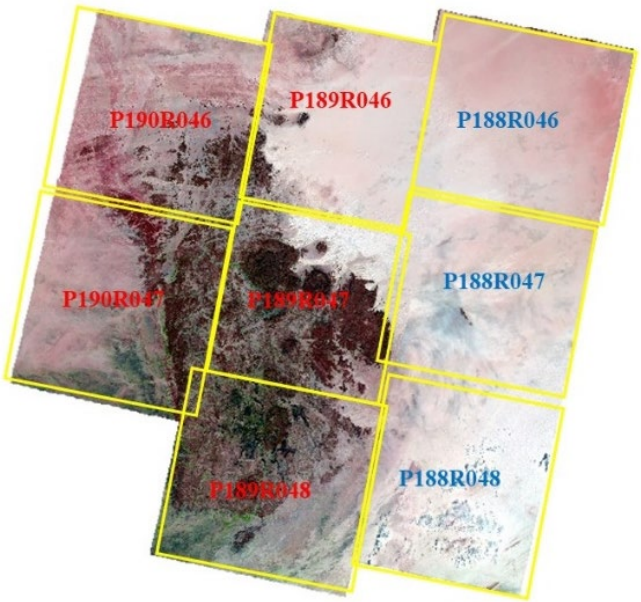


Figure 2. Mosaicking of bands.

Extraction of the Study Area

This step involves delineating a study area on a satellite image or on the set of mosaicked scenes. This operation, which follows the mosaicking process, allowed the study area to be extracted without any modification of the information contained in the images, using the shapefile from the reserve.

Classification

This is one of the steps in the statistical processing of multispectral images, which can vary in complexity. There are two types of multispectral satellite image classification: unsupervised classification and supervised classification [21]. Since supervised classification requires, a priori, a good understanding of the study area.

Field knowledge and GPS data were used to identify the various land-use classes. This supervised classification was used to convert and analyze the information from the raster images into a thematic map. Consequently, the pixels in each image were classified using the maximum likelihood algorithm, which was applied to all images from 2000, 2005, 2015, and 2025.

Post-classification

It is calculated using the following equation [22]

$$k = \frac{P_o - P_e}{1 - P_e} \quad (1)$$

where P_o is the observed proportion of agreement or observed concordance, and P_e is the proportion of random agreement or random concordance.

Table 2. Rating scale and Kappa coefficient values according to [8].

Kappa Coefficient	Ratings
0.81 - 1.00	Excellent
0.61 - 0.80	Good
0.41 - 0.60	Moderate
0.21 - 0.40	Poor
<0.00	Very poor

Overall Accuracy

Overall accuracy provides information on the overall quality of the classification [23] (**Table 2**). It correspond to the number of correctly classified pixels (pixels on the diagonal of the confusion matrix) relative to the total number of pixels the researcher is seeking to classify classification [21]. It represents the proportion of correctly classified pixels but does not provide information about the pixels in the different classes. This overall accuracy is derived from the confusion matrix, which compares pixels across different classes

$$\mathrm{PG} = \frac{\text{Total number of correct samples}}{\text{Total number of samples}} * 100 \quad (2)$$

With PG Précision Globale.

Confusion Matrix

The confusion matrix reflects the quality of the classification. It allows for a statistical comparison between the number of correctly classified pixels and the number of incorrectly classified pixels classification [23]. It is presented in the form of a contingency table. The diagonals (rows) of the matrix provide information on the thematic classes resulting from the classification procedure, and the columns correspond to the thematic classes associated with the control points classification [23]. This matrix is used to determine the Kappa coefficient (K); Global Precision; omission error; and commission error.

Omission Error (OE) and Commission Error (CE)

An omission error, or deficit error, occurs when a pixel has not been classified

into its correct class. A commission error, on the other hand, occurs when a pixel has been classified into a class that does not correspond to its correct class. Thus, the omission error appears in the columns of the confusion matrix, and the commission error appears in the rows of the confusion matrix. According to Oreste *et al.*, 2019, these two indices (EO and EC) are calculated using the following equations, respectively:

EO = 1 – IPC, where EO = omission error and IPC = Class Purity Index

And EC = 1 − ICV, where EC = commission error and ICV = the Cartographic Validation Index.

Cartographic Analysis

ENVI 5.3 software was used to delineate the study area and to vectorize (convert from raster format to shapefile) images from various years—2000, 2005, 2015, and 2025—using the Raster to Vector algorithm. The vectorized images were exported to ArcGIS 10.8 to perform various statistical calculations to validate the classification. During this process, five land-cover classes were identified for all years: rock outcrop; riparian strip; steppe; Ténéré erg; and guelta/mare.

2.6. Calculation of Landscape Transformation Indices

The identification of the landscape transformation process is defined according to the decision tree proposed by [24] and [25]. The landscape transformation identification indices take into account the number of patches, the area, and the perimeter of a class *j*. Thus, the statistical analysis of these indices strengthens the analysis of ecosystem landscape dynamics. Statistical variation in these indices from one class to another or from one year to the next can result in multiple transformations. These include aggregation (merging of patches), removal (disappearance of patches), creation (formation of new patches), deformation (change in patch shape), enlargement (expansion of patch size), perforation (formation of holes in patches), displacement (translocation of patches), shrinkage (reduction in patch size), fragmentation (break in continuity into several disjoint patches), and dissection (subdivision of patches by small-scale lines), according to [26]. Let n_o, a_o, p_o be, respectively, the number of patches, total area, and total perimeter in the initial year, and let n_1, a_1, p_1 be, in the same respective order, the number of patches, total area, and total perimeter in the final year. To distinguish between fragmentation and dissection, an observed equation time ($t_{obs} = a_1/a_0$) is calculated and compared to a predefined threshold time $t = 0.5$.

If $t_{obs} < t$, the process indicates fragmentation.

If $t_{obs} > t$, it indicates dissection

Number of patches

The number of patches in a class is the set of patches belonging to a given class j (n_j) [27] (**Figure 3**).

Total area

Total area is defined as the sum of the surface areas of all patches a_{ij} occupied by class *j*. It is expressed in square kilometers (km^2). Let a_{ij} be the area of the *i*-th

patch in class *j* [27]. It is calculated using the following formula:

$$a_{tj} = \sum_{i=1}^{n_j} a_{ij} \tag{3}$$

Perimeter of a Class

The sum of the outlines of patches *i* is the total perimeter, denoted P_{tj}, of a class *j*. It is expressed in kilometers and is calculated using the following equation

$$P_{tj} = \sum_{i=1}^{n_j} P_{ij} \tag{4}$$

With P_{ij}, the area of a class *i* within class *j*.

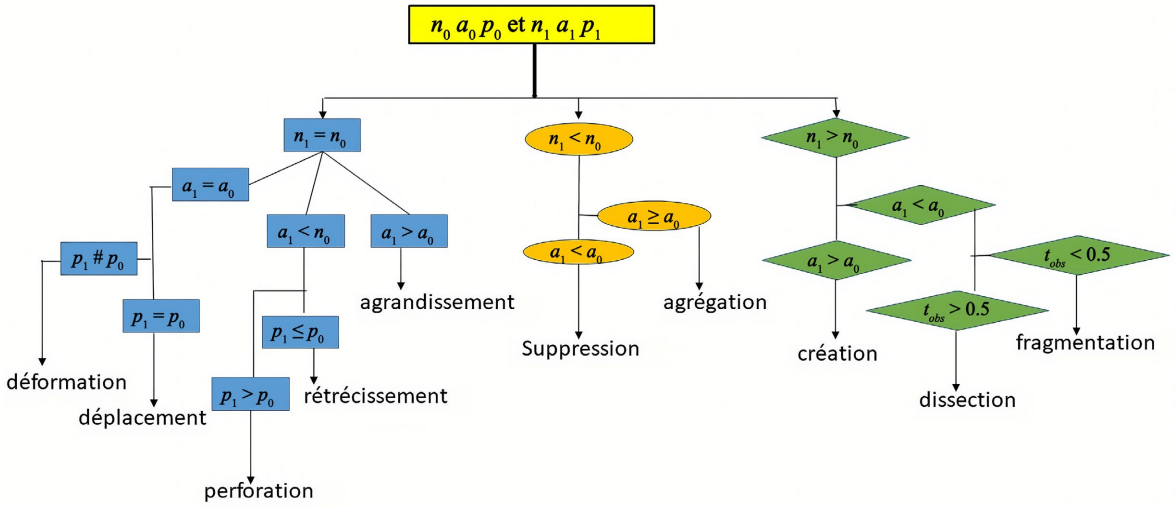


Figure 3. Decision tree proposed by Bagaert *et al.*, 2004.

2.7. Assessment of Land-Use Dynamics

2.7.1. Creation of Change Maps

The change maps were produced by combining two maps—one from the initial year and one from the final year. This combination was based on a system for comparing classes over a given period. Its purpose is to highlight the various possible changes between land-use classes. To this end, the assessment of ecosystem change processes was conducted according to three scenarios based on the rate of change in land-use classes and the degree of transition between these classes: stability, expansion, and regression [28].

2.7.2. Transition Matrix

The transition matrix highlights the landscape changes that occurred between two dates, t_0 and t_1. In this matrix, the areas of the different land-use classes are obtained by overlaying two maps from different years using the "Intersect" function in the "Arc Toolbox" menu of the ArcGIS software. This matrix consists of m rows and n columns. The number m of rows in the matrix indicates the number of landscape units that existed in the initial year, while the number n of columns in the matrix indicates the number of landscape units converted in the final year

[29].

2.8. Rate of Change in Land-Use Classes

The rate of change for the various classes was calculated to assess the impact of changes in land-use patterns on the landscape [30]. The rate of change is calculated using the following formula:

$$T = (A_2 - A_1)/A_1 \times 100 \quad (5)$$

where A_1 is the area of a land-use class in the initial year and A_2 is the area in the final year. The value of the rate of change can be positive (+), negative (−), or zero (0). Thus, when:

$T > 0$: there is an increase in the area of the land-use class from period A_1 to A_2.

$T < 0$: there is a decrease in the area from A_1 to A_2.

$T = 0$: or close to zero (0), landscape stability is observed between two maps from different years, A_1 and A_2.

Rate of Change in Land-Use Classes

To determine the rate at which land-use classes are changing, the following equation was used:

$$\Delta_s = \frac{SP_2 - SP_1}{t_2 - t_1} \quad (6)$$

where: Δ_s = Rate of change (in ha/year). Where SP_1 = Area occupied by the land-use category in question during the initial year "1" (ha); SP_2 = Area occupied by the land-use category in question during the target year "2" (ha); t_1 = initial year "1"; t_2 = target year "2" [31].

3. Results

3.1. Validation Assessment of the Classification

Five (5) land-use classes were identified based on the analysis of time-series data from Landsat satellite imagery from 2000, 2005, 2015, and 2025. The results were validated using overall accuracy indices, the Kappa coefficient, the confusion matrix, and classification errors (omission and commission). Thus, the analysis of the performance results of the classified images yielded statistically significant values. Indeed, these values are, on the whole, very similar for all years (2000, 2005, 2015, and 2025), with overall accuracies of 96.91%, 85.32%, 97.63%, and 98.26%, and Kappa coefficients of 0.95, 0.80, 0.97, and 0.98 (**Table 3**).

Table 3. Estimation of classification quality.

Landsat Images	Overall Accuracy Indices (%)	Kappa Coefficients
2000	96.91	0.95
2005	85.32	0.80
2015	97.63	0.97
2025	98.26	0.98

An analysis of the confusion matrix results reveals low confusion among the four (4) years (2000, 2005, 2015, and 2025). In 2000, the different classes identified were Rock Outcrop; Riparian Vegetation; Ténéré Erg Steppe; and Guelta/Mare, with correctly classified pixels at 99.22%, 97.87%, 88.56%, 97.37%, and 97.45%, respectively, in chronological order (Table 4). Despite these percentages of correctly classified pixels, there are still some omission errors ranging from 0.78% to 11.44% and inclusion errors ranging from 0.11% to 32.89% revealed in the classification. In 2005, the precision matrix shows that 73.05% and 87.69% of the pixels in the rock outcrop and riparian strip classes, respectively, were correctly classified. As for the steppe class—Ténéré Erg and Guelta/Mare—92.97%, 98.89%, and 98.66% of the pixels are correctly classified in the respective order of the classes (Table 5).

Table 4. Confusion matrix and classification errors (false positives and false negatives) for the 2000 images.

Classes 2000	Riparian	Erg	Steppe	Rock outcrop	Guelta/ Pond	Errors of Commission
Riparian	97.87	0.00	6.12	0.03	0.00	2.13
Erg	0.27	97.37	5.20	0.01	0.00	2.63
Steppe	1.69	2.63	88.56	0.08	0.00	11.44
Rock outcrop	0.16	0.00	0.12	99.22	2.55	0.78
Guelta/Pond	0.00	0.00	0.00	0.66	97.45	2.55
Errors of commission	12.45	1.96	8.48	0.11	32.89	

Table 5. Confusion matrix and false positive and false negative errors in the 2005 images.

Classes 05	Rock outcrop	Riparian zone	Steppe	Erg of Ténéré	Guelta/ Pond	Erreur of commission
Rock outcrop	73.05	2.46	1.26	4.78	2.44	26.95
Riparian zone	0.20	87.69	4.87	0.00	0.00	12.31
Steppe	2.81	9.56	92.97	1.53	1.83	7.03
Erg of Ténéré	0.28	0.21	0.06	93.69	0.00	6.31
Guelta/Pond	23.66	0.07	0.84	0.00	95.73	4.27
Errors of commission	6.79	7.08	22.18	0.38	91.53	

However, classification errors ranging from 6.31% to 26.95% and commission errors ranging from 0.38% to 91.53% are present in the classification. Furthermore, in 2015, 98.54%, 90.65%, 95.30%, 93.69%, and 98.66% of the pixels were correctly classified, as shown by the confusion matrix for the respective classes: rock outcrop; riparian strip; steppe; Ténéré erg; and guelta/mare. Nevertheless, classification errors exist, notably omission errors ranging from 1.11% to 9.35% and commission errors ranging from 0.28% to 19.93% (Table 6). Finally, in 2025, the classification confusion matrix showed that 97.84% - 98.32% of the pixels are

correctly classified into their respective classes (rock outcrop and riparian strip) and 96.82% - 99.92% - 100.00% are correctly classified into the steppe class, respectively; Ténéré Erg and Guelta/Mare (Table 7). Furthermore, the confusion matrix revealed a few classification errors. These include omission errors ranging from 0.00% to 3.18% and commission errors ranging from 0.00% to 47.37%.

Table 6. Confusion matrix and false positive and false negative errors for the 2015 images.

Classes 15	Rock outcrop	Riparian zone	Steppe	Erg of Ténéré	Guelta/ Pond	Errors of commission
Rock outcrop	98.54	0.42	0.31	0.00	0.45	1.46
Riparian zone	0.25	90.65	4.09	0.02	0.89	9.35
Steppe	0.12	8.78	95.30	1.09	0.00	4.70
Erg of Ténéré	0.00	0.00	0.00	98.89	0.00	1.11
Guelta/Pond	1.06	0.14	0.31	0.00	98.66	1.34
Erreur of commission	0.28	15.90	4.37	0.00	19.93	

Table 7. Confusion matrix and false positive and false negative errors for the 2025 images.

Classes 25	Rock outcrop	Riparian zone	Steppe	Erg of Ténéré	Guelta/ Pond	Erreur of commission
Rock outcrop	97.84	0.28	0.00	0.00	0.00	2.16
Riparian zone	1.38	98.32	3.18	0.00	0.00	1.68
Steppe	0.00	1.40	96.82	0.08	0.00	3.18
Erg ofTénéré	0.00	0.00	0.00	99.92	0.00	0.08
Guelta/Pond	0.78	0.00	0.00	0.00	100.00	0.00
Erreur of commission	0.35	3.63	1.83	0.00	47.37	

3.2. Trends in Land Cover Composition from 2000 to 2025

The analysis of the time series of Landsat-category satellite images involved mapping five (5) land-use classes for the years 2000, 2005, 2015, and 2025. The descriptive characteristics of the different classes are listed in Table 8.

Table 8. Characteristics of land-use units.

Land-use classes	Characteristics of the Classes
Rock outcrop	Rocky area featuring large mountain ranges, hills, and often rocky plains. The dominant species in this class are: Acacia ehrenbergiana;
Riparian zone	Vegetation found along wadis/koris: Vachellia tortilis subsp.; Calotropis procera (Aiton) W.T. Aiton; Prosopis juliflora (Sw) DC. In irrigated agricultural areas, one finds Phoenix dactylifera L.; Citrus sinensis L.; and Allium cepa L.
Steppe	An area dotted with species of the genera Aristida, Stipagrostis, Panicum turgidum Forssk, and Schouwia thebaica Webb. These often coexist with a few clumps of Acacia ehrenbergiana shrubs.

Continued

Erg of Ténéré	A vast desert region dominated by shifting sand dunes.
Guelta/Pond	An area saturated with water in a rocky depression or a generally temporary water source in valley depressions.

For illustrative purposes, Figure 4 provides an overview of certain classes of RNNAT (Figure 5).



(A) (B) (C)

Figure 4. Illustration of RNNAT land-use categories, with (A) Riparian forest, (B) Steppe, and (C) Rocky outcrop.

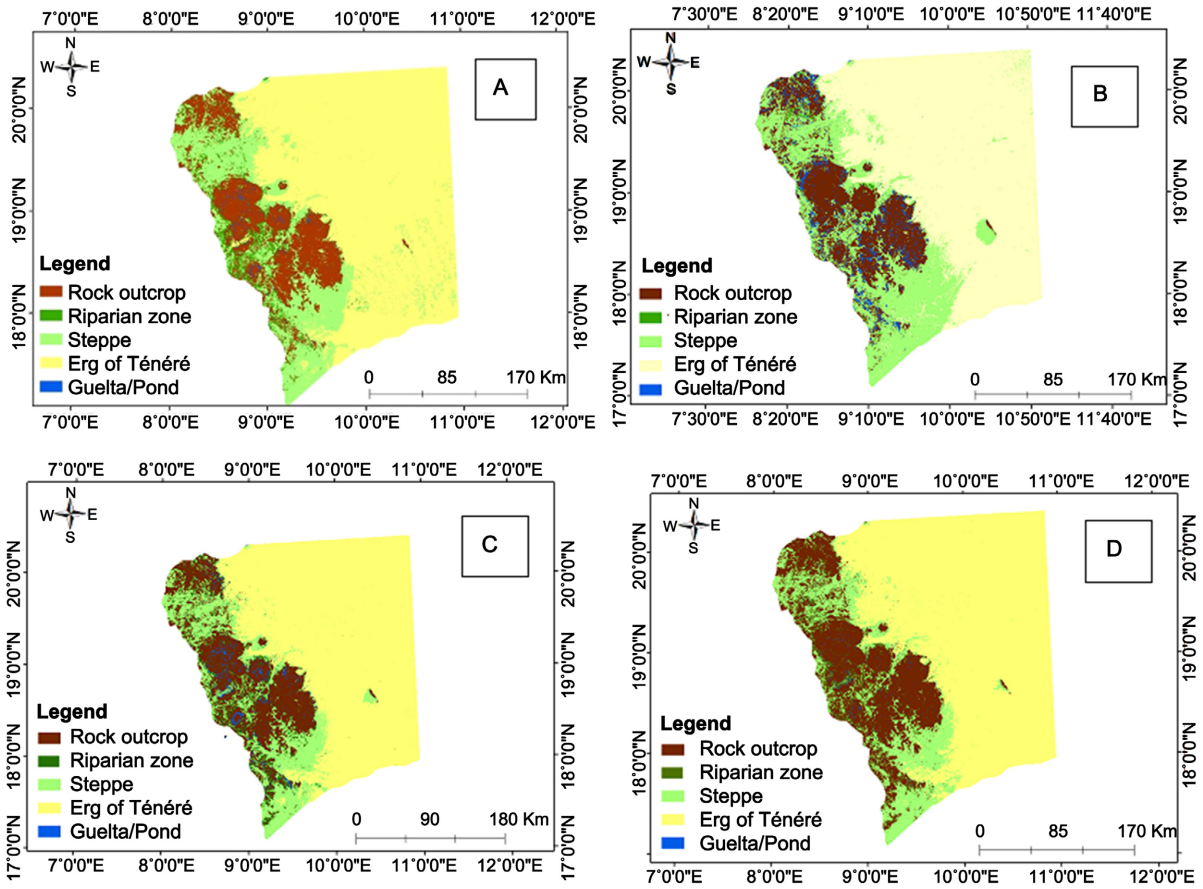


Figure 5. The various land-use maps, with (A) 2000 map; (B) 2005 map; (C) 2015 map; and (D) 2025 map.

3.3. Landscape Conditions

Analysis of the land-use classes in the RNNAT landscape reveals that the Ténéré Erg class is the most dominant, accounting for 62.04%, 58.53%, 63.28%, and

62.52% of the total area in 2000, 2005, 2015, and 2025, respectively. This class accounts for nearly two-thirds of the study area's landscape. The steppe class covers 19.20% of the area in 2000 and 22.80% in 2005. Next is the rocky outcrop class, which covers 14.54% of the area in 2000 and 16.06%; 18.62% in 2015 and 2025, respectively. The rocky outcrop class is followed by the riparian strip class, which covers a larger area than the Guelta class, with 3.82%, 11.22%, 14.81%, and 15.38% of the total area in 2000; 2005, 2015, and 2025, respectively. Furthermore, the Guelta class accounts for a smaller area in 2000, 2005, 2015, and 2025, at 0.40%, 0.73%, 1.00%, and 0.27%, respectively (Figure 6). Thus, the areas in hectares (ha)—the source of these percentage values—are listed in Table A1 in the **Appendix**.

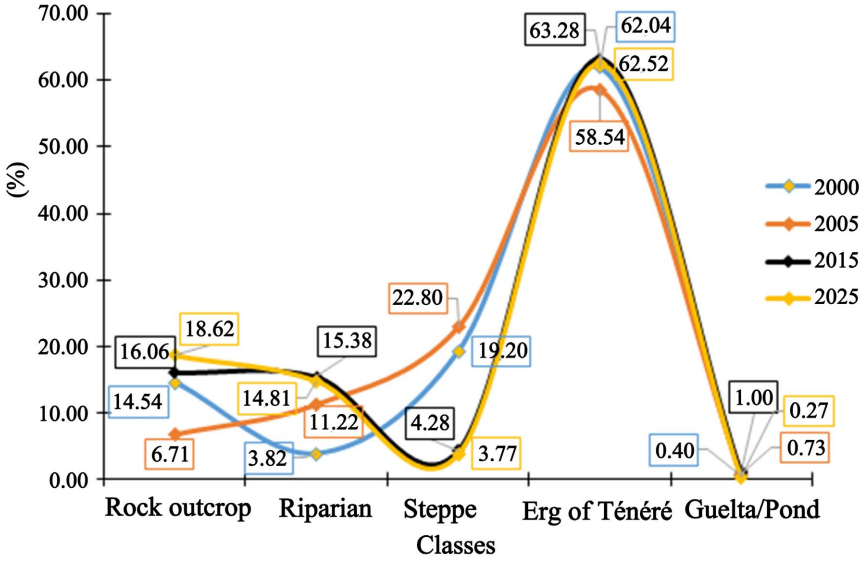


Figure 6. Parentage of area by land-use class.

3.4. Rates of Ecosystem Change

An analysis of Table 9 shows that between 2000 and 2005, the riparian zone, steppe, and Guelta/Mare classes experienced positive rates of change, with values of 1.94, 0.19, and 0.84. However, the "Rock Outcrop" and "Ténéré Erg" classes experienced negative rates of change of −0.54 and −0.06, respectively. From 2005 to 2015, all classes (Rock Outcrop, Riparian Belt, Ténéré Erg, and Guelta/Mare) showed positive growth rates of 1.39, 0.37, 0.08, and 0.36, respectively, except for the Steppe class, which had a growth rate of −0.81. Between 2015 and 2025, only the "Rock Outcrop" class experienced a progressive change at a rate of 0.16. The "Riparian Forest," "Steppe," "Ténéré Erg," and "Guelta/Mare" classes all underwent regression, with respective rates of change of −0.04; −0.12; −0.01; and −0.73.

3.5. Analysis of Spatial Structure Dynamics

An analysis of Table 10 reveals that the highest number of patches was observed in the "Steppe" class in 2025, with 411,005 patches, followed by the "Riparian Strip" class in 2000, with 269,305 patches. Thus, the "Rock Outcrop," "Ténéré

Erg," and "Guelta/Mare" classes had higher numbers of patches in 2005 compared to other years. These numbers of patches were 210,225, 96,459, and 191,164, respectively, in 2005. Furthermore, the number of patches (n_j) and the perimeter (p_j) and area (a_j) indices in Table 10 were used to determine the spatial transformation process of the reserve (Table 11). The analysis of the table reveals that four (4) transformations were recorded between 2000 and 2005. Indeed, when classified according to the different land-use categories, the rocky outcrop class underwent fragmentation because the area of the patches in the initial year (2000) was greater than that in the final year (2005) and that $t_{obs} = 0.4 < 0.5$. Next, the dissection phenomenon is recorded by the Ténéré Erg class, since $t_{obs} = 0.9 > 0.5$. However, one aggregation is known to have occurred in the Riparian Vegetation and Steppe class. The Guelta/Mare class underwent a reorganization because the number of patches and the total perimeter of the 2000 class were smaller than those of 2005. During the 2005-2015 period, three (3) spatial transformations were observed. This involves the aggregation process occurring within the "Rock Outcrop" class, which is repeated in the "Ténéré Erg" and "Guelta/Mare" classes, as their areas in 2005 were smaller than those in 2015. Next, fragmentation ($T_{obs} = 0.18$) occurred in the Steppe class, while new areas were created in the Riparian Forest class. During the 2015-2025 period, four (4) landscape transformations were again recorded. Thus, from 2015 to 2025, the Riparian Forest and Steppe classes—which were expected to harbor significant vegetation—all underwent fragmentation because $t_{obs} > 0.5$. Furthermore, the Ténéré Erg class also experienced fragmentation ($t_{obs} = 0.9$ and $t_{obs} = 0.8$, respectively). Thus, the Erg du Ténéré class also underwent a dissection with $t_{obs} = 0.9 < 0.5$. However, the "Rock Outcrop" and "Guelta/Mare" classes underwent aggregation and removal, respectively (the number of patches and the area in the initial year were greater than those in the final year).

Table 9. Rates of change for land-use units within the same class.

Classes	Rate of change between classes		
	2005-2000	2015-2005	2025-2015
Rock outcrop	−54	139	16
Riparian zone	194	37	−4
Steppe	19	−81	−12
Erg of Ténéré	−6	8	−1
Guelta/Pond	84	36	−73

Table 10. Spatial structure indices.

Years	Indices	Rock outcrop	Riparian zone	Steppe	Erg of Ténéré	Guelta/Pond
2000	N_j	72,198	269,305	262,032	86,370	77,702
	a_j (km^2)	11110.81	2918.02	14671.62	47409.87	305.17
	p_j (km)	73870.76	100142.34	149833.33	59490.97	17736.78

Continued

2005	N_j	210,225	151,731	223,873	96,459	191,164
	a_j (km^2)	5129.54	8570.32	17424.29	44730.82	560.49
	p_j (km)	98163.01	132691.76	137714.35	55562.49	32526.87
2015	N_j	116237	184324	404689	37807	116616
	a_j (km^2)	12271.90	11756.26	3269.86	48354.19	762.82
	p_j (km)	100315.66	108135.17	138479.41	35828.80	31863.66
2025	N_j	106,761	204,514	411,005	38,834	100,572
	a_j (km^2)	14231.76	11319.84	2883.36	47771.48	208.65
	p_j (km)	90687.75	120103.30	126449.44	39275.88	17827.16

1

Table 11. Spatial patterns obtained after the exercise.

Classes	Themes	Period (2000-2005)	Period (2005-2015)	Period (2015-2025)
Rock outcrop	N_j	nt2000< nt2005	nt2005 >nt2015	nt2015 > nt2025
	A	a2000 > a2005	a2005 <a2015	a2015 < a2025
	Transformation	T_{obs} = 0.4 **Fragmentation**	**Agrégation**	**agrégation**
Riparian zone	N_j	nt2000 > nt2005	nt2005 < nt2015	nt2015 < nt2025
	A	a2000 < a2005	a2005 < a2015	a2015 > a2025
	Transformation	**Agrégation**	**Création**	T_{obs} = 0.9 > 0.5 **dissection**
Steppe	N_j	nt2000 > nt2005	nt2005 < nt2015	nt2015< nt2025
	A	a2000 < a2005	a2005 > a2015	a2015 > a2025
	Transformation	**Agrégation**	T_{obs} = 0.18 < 0.5 **fragmentation**	T_{obs} = 0.8 > 0.5 **dissection**
Erg of Ténéré	N_j	nt2000 < nt2005	nt2005 >nt2015	nt2015 < nt2025
	A	a2000 > a2005	a2005 < a2015	a2015> a2025
	Transformation	T_{obs} = 0.9 > 0.5 **dissection**	**Agrégation**	t_{obs} < 0.5 **dissection**
Guelta/Pond	N_j	nt2000 <nt2005	nt2005 >nt2015	nt2015 > nt2025
	A	a2000 <a2005	a2005< a2015	a2015 > a2025
	Transformation	**Création**	**Agrégation**	**suppression**

3.6. Transition Matrices

The dynamics of land-use categories between 2000 and 2005, 2005 and 2015, and 2015 and 2025 are presented in Tables 12-14. Thus, transitions occur from the columns to the rows, and the diagonals represent the areas of classes that have remained stable, while the classes outside the diagonal correspond to changes from one land-use class to another.

Table 12. Transition matrix from 2000 to 2005.

Classes	Rock outcrop	Riparian zone	Steppe	Erg of Ténéré	Guelta/Pond	Total
Rock outcrop	60.50	0.03	0.74	2.7E−03	38.72	100.00
Riparian zone	18.30	6.79	61.71	9.5E−02	13.10	100.00
Steppe	8.21	2.72	80.03	8.8E+00	0.26	100.00
Erg of Ténéré	0.24	0.01	7.89	9.2E+01	0.26	100.00
Guelta/Pond	1.87	0.01	0.27	7.3E−02	97.78	100.00

Table 13. Transition matrix from 2005 to 2015.

Classes	Rock outcrop	Riparian zone	Steppe	Erg of Ténéré	Guelta/Pond	Total
Rock outcrop	90.58	6.43	1.93	0.75	0.31	100.00
Riparian zone	1.59	51.43	46.75	0.11	0.12	100.00
Steppe	2.52	12.20	63.37	21.86	0.04	100.00
Erg of Ténéré	0.01	0.05	0.49	99.45	0.00	100.00
Guelta/Pond	77.60	6.61	1.07	0.00	14.72	100.00

Table 14. Transition matrix from 2015 to 2025.

Classes 15 - 25	Rock outcrop	Riparian zone	Steppe	Erg of Ténéré	Guelta/Pond	Total
Rock outcrop	99.47	0.28	0.06	1.5E−04	0.19	100.00
Riparian zone	38.81	48.61	10.15	1.5E−01	2.29	100.00
Steppe	0.90	10.71	84.12	4.2E+00	0.04	100.00
Erg of Ténéré	0.00	0.01	2.24	9.8E+01	0.00	100.00
Guelta/Pond	78.96	5.08	0.08	0.0E+00	15.87	100.00

Analysis of the transition matrix (Table 12) shows that all land-use classes observed in 2000 were still present in 2005. Nevertheless, some transition percentages between classes are noted. A closer examination of the statistics in Table 12 reveals that between 2000 and 2005, the most significant transitions occurred from the "Rock Outcrop" class to "Guelta/Mare" and from the "Riparian Strip" class to "Steppe," at 38.72% and 61.71%, respectively. However, the Steppe, Ténéré Erg, and Guelta/Mare classes remained virtually stable, with respective percentages of 80.03%, 92%, and 97.78%. Furthermore, within the transition matrix for 2005 and 2015 (Table 13), the same land-use classes recur but differ in their transition trends and statistics. The most notable transitions are observed in the conversion of 46.75% of riparian forest to steppe, followed by steppe to Ténéré erg and guelta/mare to rocky outcrop, at 21.86% and 77.60%, respectively. In contrast, the more or less stable classes are: the rocky outcrop class (90.58%) and the Ténéré Erg (99.45%). An examination of the transition matrix for 2015 and 2025 (Table

14) reveals that the Guelta/Mare class is largely converted to rocky outcrop, with a high transition value of 78.96%. Furthermore, this conversion between the different land-use categories occurred from the Riparian Strip class to Rock Outcrop and from Steppe to Riparian Strip, at rates of 38.81% and 10.71%, respectively. However, it should be noted that the "Rock Outcrop" and "Ténéré Erg" classes have stability rates of 99.47% and 98%, respectively.

3.7. Rate of Ecosystem Change

The rates of ecosystem change calculated over a 25-year period are listed in Table 15. An analysis of Table 15 shows that between 2000 and 2005, the rates of change for the Riparian Forest, Steppe, and Guelta classes increased by 113,046.14 ha/year, 55053.54 ha/year, and 5106.41 ha/year, respectively. However, the "Rock Outcrop" (−119625.46 ha/year) and "Ténéré Erg" (−53580.94 ha/year) classes experienced a decline in their rate of change. Furthermore, between 2005 and 2015, only the Steppe class experienced a decreasing rate of change of −141544.31 ha/year. In contrast, the land-use units, notably: Rocky Outcrops; Riparian Forest; Ténéré Erg; and Guelta—all experienced an increasing rate of 71423.63 ha/year; 31859.39 ha/year; 36233.71 ha/year; and 2023.35 ha/year, respectively. Between 2015 and 2025, the same trend of decreasing rates is still observed in the land-use categories (riparian zone; steppe; Ténéré ergs and gueltas), with the exception of the "rock outcrop" category. These land-use units have decreasing rates of change of −4364.23 ha/year, −3865.03 ha/year, −5827.11 ha/year, and −5541.76 ha/year, respectively, while the Rocky Outcrop class has an increasing rate of change of 19598.60 ha/year.

Table 15. Rate of change of ecosystems.

Classes	Vitesse du changement des classes		
	2000 à 2005 (ha/ans)	2005 à 2015 (ha/ans)	2015 à 2025 (ha/ans)
Rock outcrop	−119625.46	71423.63	19598.60
Riparian zone	113046.14	31859.39	−4364.23
Steppe	55053.54	−141544.31	−3865.03
Erg of Ténéré	−53580.94	36233.71	−5827.11
Guelta/Pond	5106.41	2023.35	−5541.76

4. Discussion

The results of the validation of the various land-use classes revealed that the overall accuracy indices (96.91%; 85.32%; 97.63%; and 98.26%) and the Kappa coefficients (0.95; 0.80; 0.97; and 0.98) are satisfactory. Thus, these results highlight that there is good agreement among the land-use classes. This agreement may be due to the images being acquired under clear-sky conditions. The ground-truth data, combined with the high image quality, facilitated the comparison and visual interpretation of the images. This point has been emphasized by several authors,

including [21]. The Kappa coefficient of 0.80, compared to the other coefficients, may be due to the scratch corrections applied to the 2005 images. However, analyses of the confusion matrices reveal that certain land-use classes are not clearly distinguishable from one another. This could be related to the very close similarity of their spectral signatures., reached the same conclusion [32] and [33].

An analysis of the areas covered by the various land-use classes shows that the landscape of the RNNAT is dominated by the Ténéré Erg class, which accounted for 62.04%, 58.53%, 63.28%, and 62.52% of the total area in 2000, 2005, 2015, and 2025, respectively. These percentages show that this class accounts for nearly two-thirds of the study area's landscape. This proportion has already been highlighted by several authors, notably [5] and [7]. This dominance of the Ténéré Erg could be linked to the RNNAT's proximity to the greater Sahara. This class is followed by the Steppe class, which dominated between 2000 and 2005; between 2015 and 2025, the Riparian Forest class dominated the Steppe class. This decline in the Steppe class in favor of the Riparian Forest class between 2015 and 2025 could be due to a return of rainfall in the Sahelian zone during this period [34]-[37]. This observation has been made by several authors. However, this phenomenon differs from what was observed by [38], who found that the shrubby steppe is giving way to the grassy steppe. This difference could be linked to the extreme rarity of bushfires in the RNNAT. However, the Guelta/Mare class is underrepresented in all years. This could be due to the scarcity of rainfall in semi-arid and arid ecosystems or related to the months in which the images were captured.

An analysis of ecosystem change rates shows that between 2000 and 2005, the riparian zone, steppe, and Guelta/Mare classes experienced positive change rates of 194%, 19%, and 84%, respectively. This could be due to a reduction in anthropogenic pressure. However, the "Rock Outcrop" and "Ténéré Erg" classes experienced negative change rates of −54% and −6%, respectively. This decline in these classes could be due to a prolonged drought. From 2005 to 2015, all classes (Rock Outcrop, Riparian Strip, Ténéré Erg, Guelta/Mare) showed positive trends with respective rates of 139%, 37%, 8%, and 36%, except for the Steppe class, which showed a rate of −81%. The respective rates of change—139%, 37%, 8%, and 36%—could be due to a return of favorable rainfall conditions in the area. As for the decline in the Steppe class, it could be due to intensive grazing or soil degradation. Between 2015 and 2025, only the Rocky Outcrop class experienced a gradual increase of 16%. The Riparian Forest, Steppe, Ténéré Erg, and Guelta/Mare classes all experienced a decline, with respective rates of change of −4%, −12%, −1%, and −73%. This decline in these four (4) classes could be attributed to demographic pressure or a lack of significant regeneration.

Analysis of the spatial transformation process revealed five (5) processes over the entire period from 2000 to 2025. These include, among others, aggregation; creation; fragmentation; dissection; and removal. Between 2000 and 2005, the phenomena of fragmentation and dissection were observed, respectively, in the rock outcrop class and the Ténéré Erg. These two phenomena may be due to min-

ing activities and overgrazing in the RNNAT and its surrounding areas. These two processes—the disruption of continuity or the subdivision of patches—have a negative impact on biodiversity. These two processes of spatial transformation were reported by [39] in the RPFD. Furthermore, aggregation was observed in the riparian forest and steppe classes. This explains the merging of patches within these classes. This phenomenon could be due to vegetation regeneration following years of severe drought or to the extensive efforts made by managers to restore lands within the RNNAT. This form of transformation is documented by [26] and [38] in classified forests and the RGB, respectively.

In contrast, a formation process is observed in the Guelta/Mare class. This could be due to a return of rainfall or to the fact that the Guelta are not silted up.

Between 2005 and 2015, the formation process was observed for the riparian cordon class. This reflects an expansion of the riparian cordon class. This process could also be due to a partial increase in cumulative rainfall in arid and semi-arid areas. Reference [36] reached the same conclusion. This could also be attributed to the "barra" systems (spillways in certain koris) that regulate water flow within the koris. [39] and [40] reported the same findings regarding the functioning of these spillways. However, the steppe class underwent fragmentation during this period. This could be linked to a prolonged drought or overgrazing in grassy areas. Furthermore, the rock outcrop, Ténéré Erg, and Guelta/Mare classes all underwent aggregation. This could be explained by a retreat of the steppe class. Between 2015 and 2025, the riparian forest, steppe, and Ténéré Erg classes underwent a process of dissection. This transformation process within these various classes could be due to the ecologically unfavorable arid conditions of the environment or be explained by the massive presence of vehicles crossing the RNNAT in search of gold within the reserve and its surrounding areas toward the end of 2014. From 2014 to the present, there has continued to be a massive influx of people into several areas of the RNNAT. By 2025, there were up to 13 gold mining and prospecting sites within the RNNAT. It should be noted that prospecting continued in the RNNAT and its surrounding areas until 2026, despite the decree classifying the reserve. In fact, mining operations are largely unregulated and destructive. As a result, several gold pits have been established in the heart of the valleys. Thus, the phenomenon of aggregation is repeated within the fractured rock outcrop. Furthermore, aggregation has been observed within the rock outcrop itself. This decline could be attributed to low precipitation in the Saharan region, combined with high evaporation rates.

An analysis of land-use dynamics revealed five (5) land-use classes across all time periods: 2000-2005, 2005-2015, and 2015-2025. Furthermore, these classes did not undergo a complete conversion. However, some classes show a certain percentage of transition between them. Consequently, between 2000 and 2005, the most pronounced transitions were observed between the "Rock Outcrop" to "Guelta/Mare" and "Riparian Belt" to "Steppe" classes, at 38.72% and 61.71%, respectively. The transition from "Rock Outcrop" to "Guelta/Mare" could be ex-

plained by the similarity of their pixels, as gueltas are water sources located on plateaus. The transition from "Riparian Belt" to "Steppe" results in a reduction in woody vegetation cover. This transition could be linked to recurring droughts in Sahelo-Saharan ecosystems. Between 2005 and 2015, the Riparian Forest class underwent a further 46.75% conversion to Steppe, followed by a conversion from Steppe to Ténéré Erg. This could be explained by the shift of nomadic herders toward agro-pastoralism. This agricultural practice often involves clearing land in alluvial valleys (riparian strips) to create irrigated plots. In fact, most of these plots are bordered by dead hedgerows of acacia and *Prosopis juliflora*. Between 2015 and 2025, the riparian strip land use class transitioned to the rocky outcrop land use class. This transition may be attributed to mining activities on the plateaus in particular. In fact, any tree located along a gold vein will be cut down or uprooted, regardless of its value as a source of firewood. This decline of riparian groves in favor of steppes is supported by [41]. In contrast, the Guelta/Mare class consists largely of rocky outcrops (78.96%). This could still be related to droughts or pixel classification errors.

An analysis of the rate of ecosystem change shows that between 2000 and 2005, the Riparian Forest, Steppe, and Guelta classes gradually expanded. This rate of change for these classes could be linked to the lack of increasing human activities within the RNNAT. Furthermore, between 2005 and 2015, only the Steppe class experienced a decline. This decline could be linked to overgrazing in grassy habitats. Between 2015 and 2025, all classes experienced a decline in rate except for the Rocky Outcrop class. The decreasing rate of decline across the classes during the 2015-2025 period could still be attributed to the surge in mining and other human activities, such as vegetable farming, which depletes the water table through excessive pumping. This finding is supported by the observations in [42]-[45].

5. Conclusions

This study, conducted in the Aïr and Ténéré National Nature Reserve (RNNAT) using remote sensing and Geographic Information Systems (GIS), combined with field data, enabled a qualitative and quantitative analysis of landscape changes based on land-use maps from 2000; 2005, 2015, and 2025.

The cartographic analysis reveals that five (5) land-use units were identified. These include the following classes: rocky outcrops; riparian strips; steppe; Ténéré erg; and guelta/mare. Thus, the Ténéré Erg is the dominant ecosystem class in the RNNAT, covering 62.04%, 58.53%, 63.28%, and 62.52% of the total area in 2000, 2005, 2015, and 2025, respectively. This class is followed by rocky outcrops, which accounted for 14.54% of the area in 2000 and 16.06% and 18.62% in 2015 and 2025, respectively. Furthermore, the steppe and riparian strip classes rank third and fourth, respectively. However, the Guelta/Mare class is underrepresented in all years—2000, 2005, 2015, and 2025—at 0.40%, 0.73%, 1.00%, and 0.27%, respectively. The spatial structure analysis revealed five (5) categories of spatial transformation over the 25-year period. These include fragmentation, dissection,

aggregation, creation, and elimination. Between 2000 and 2005, the "Rock Outcrop" and "Ténéré Erg" classes underwent fragmentation and dissection, respectively. However, the Riparian Forest and Steppe classes all underwent aggregation, and the Guelta/Mare class underwent creation during the same period. Between 2005 and 2015, the aggregation process was observed in the Rock Outcrop, Ténéré Erg, and Guelta/Mare classes. Subsequently, fragmentation occurred in the Steppe class, and new formations emerged in the Riparian Forest class. Between 2015 and 2025, the Riparian Forest and Steppe classes both underwent dissection. In contrast, the Rock Outcrop classes; Ténéré Erg, and Guelta/Mare classes underwent the processes of aggregation, fragmentation, and suppression, respectively. Analysis of the transition matrices reveals that the most significant transitions were observed in the Rock Outcrop and Riparian Belt classes, at 38.72% and 61.71%, respectively, between 200 and 2005. Between 2005 and 2015, the most significant conversion occurred in the Riparian Forest class (46.75%), followed by Steppe and Guelta/Mare, at 21.86% and 77.60%, respectively. Between 2015 and 2025, the Guelta/Mare class was largely converted to rocky outcrops, with a high transition rate of 78.96%. The transition rates for Riparian Forest and Steppe were 38.81% and 10.71%, respectively. Analysis of ecosystem change rates showed that between 2000 and 2005, the Riparian Forest, Steppe, and Guelta/Mare classes experienced positive change rates with respective values of 1.94, 0.19, and 0.84. However, the Rocky Outcrop and Ténéré Erg classes showed negative rates of change of −0.54 and −0.06, respectively. From 2005 to 2015, all classes (Rocky Outcrop, Riparian Forest, Ténéré Erg, and Guelta/Mare) experienced an increase at rates of 1.39; 0.37, 0.08, and 0.36, respectively, except for the Steppe class, which showed a rate of −0.81. Between 2015 and 2025, only the Rock Outcrop class showed a progressive change at a rate of 0.16. All the others (riparian forest; steppe; Ténéré ergs; and guelta/mare) experienced a decline, with respective rates of change of −0.04, −0.12, −0.01, and −0.73. In light of these results, it is clear that the natural ecosystems of the RNNAT have experienced a decline caused by human activities (large-scale gold panning, overgrazing, and unregulated occupation of irrigated plots) during the 2015-2025 period. Thus, it is urgent to take appropriate measures to reverse the current trend in the RNNAT.

Author Contributions

Adamou Hamadou Wankoye, Abdoulaye Abdou Siradji (data collection and processing, drafting), Ali Ado and Josiane Seghieri (data analysis, proofreading, and refinement of the methodology).

Conflicts of Interest

The authors declare no conflicts of interest regarding the publication of this paper.

References

[1] Doumenge, C. (2021) Biodiversity Protection: A Look Back at the Evolution of

"Protected Areas" Around the World. https://www.cirad.fr/les-actualites-du-cirad/actualites/2021/biodiversite-et-evolution-des-aires-protegees-dans-le-monde

[2] Dudley, N. (2008) Guidelines for Applying Management Categories to Protected Areas. https://portals.iucn.org/library/efiles/documents/paps-016-fr.pdf

[3] Lecerf, R. (2008) Monitoring Anthropogenic and Climate-Induced Changes in Land Cover and Land Use at the Regional Scale Using Medium-Resolution Remote Sensing. http://journals.openedition.org/echogeo/14933

[4] Fournier, A., Sinsin B. and Mensah, G.A. (2007) What Kinds of Protected Areas for West Africa? IRD Éditions. https://books.openedition.org/irdeditions/8001?lang=en

[5] Giazzi, F. and Morel, A. (2003) Conservation et développement dans la réserve naturelle nationale de l'aïr et du ténéré (Niger), Site Du Patrimoine Mondial. *Espaces tropicaux*, **18**, 179-190. https://doi.org/10.3406/etrop.2003.1119

[6] Anthelme, F., Waziri Mato, M., de Boissieu, D. and Giazzi, F. (2006) Degradation of Plant Resources due to Human Activities and Conservation Prospects in the Aïr Mountains (Sahara, Niger). *VertigO—La Revue en Sciences de l'Environnement*, **7**, 1-12.

[7] Giazzi, F., Ciofolo, I. and Alvès, K. (2006) La réintroduction de l'autruche du Niger (Struthio camelus camelus), un projet de développement et de conservation durable dans la Réserve Aïr-Ténéré (massif de l'Aïr-Niger). *Revue de Géographie Alpine*, **94**, 7-16. https://doi.org/10.3406/rga.2006.5586

[8] Landis, J.R. and Koch, G.G. (1977) The Measurement of Observer Agreement for Categorical Data. *Biometrics*, **33**, 159-174. https://doi.org/10.2307/2529310

[9] Tahirou, H.Y., Bachirou, H.Y., Kader, M.I.A., Bassara, H.S., Bouba, H., Amadou, A. T. and Zibo, G. (2024) Impacts de l'exploitation minière aurifère sur les composantes biophysiques de l'environnement à Aouzegueur dans la commune rurale de Tabelot (Agadez, Nord-Niger). *International Journal of Innovation and Scientific Research*, **75**, 171-186. https://ijisr.issr-journals.org/abstract.php?article=IJISR-24-248-01

[10] Grégoire, E. and Gagnol, L. (2017) Ruées vers l'or au Sahara: L'orpaillage dans le désert du Ténéré et le massif de l'Aïr (Niger). *EchoGéo*, 1-22. https://www.researchgate.net/publication/317142564_Ruees_vers_l'or_au_Sahara_l'orpaillage_dans_le_desert_du_Tenere_et_le_massif_de_l'Air_Niger

[11] Bruneau de Miré, P. and Gillet, H. (1956) Contribution à l'étude de la flore du massif de l'aïr (3e Partie). *Journal d'Agriculture Tropicale et de Botanique Appliquée*, **3**, 857-886. https://doi.org/10.3406/jatba.1956.2353

[12] UICN (2010) Parcs et réserves du Niger: Evaluation de l'efficacité de la gestion des aires protégées. https://iucn.org/fr/resources/publication/parcs-et-reserves-du-niger-evaluation-de-lefficacite-de-la-gestion-des-aires

[13] Morel, A. and Giazzi, F. (2001) Y-a-t-il une spécificité montagnarde du massif de l'Aïr, au sud du Sahara? *Espaces Tropicaux*, **16**, 263-270. https://doi.org/10.3406/etrop.2001.1038

[14] Karimoune, S., Tanko Sidi, O.K. and Issiaka, H. (2017) Variabilités climatiques et évolution de l'occupation des sols dans l'oasis de Timia, Région d'Agadez, Niger. *International Journal of Tropical Geology, Geography and Ecology*, **41**, 359-374. https://www.researchgate.net/publication/323475552_Climate_variabilities_and_evolution_of_soil_occupation_in_the_Timia_oasis_in_the_Agadez_Region_Niger

[15] Emmanuel Quéré (2005) Methodological Guide for Implementing Vegetation Monitoring in Natura 2000 Sites.

https://www.cbnbrest.fr/pmb_pdf/CBNB_2005_Quere_2593.pdf

[16] Marega, O., Emeterio, J.S., Fall, A. and Andrieu, J. (2021) Remote Sensing Mapping of Vegetation Land Cover Change with Regard to Rainfall Variability in the Sahel: A Multiscale Approach. *Physio-Géo*, **16**, 1-28. https://doi.org/10.4000/physio-geo.11977

[17] Omar, M. and Abdelkader, S. (2025) The Role of GIS and Remote Sensing in Tracking Vegetation Cover in the Tlagh and El-Abed Basins (Northeastern Morocco) from 1986 to 2018. *E3S Web of Conferences*, **607**, 1-8. https://doi.org/10.1051/e3sconf/202560704020

[18] Adjonou, K., Bindaoudou, I.A., Idohou, R., Glele-kakaï, R. and Kokou, K. (2019) Satellite Monitoring of the Spatiotemporal Dynamics of Land Use in the Mono Transboundary Biosphere Reserve between Togo and Benin from 1986 to 2015. https://hal.science/hal-02174848/

[19] Yaya, I.M. and Moumouni, I. (2016) Mapping the Dynamics of Forest Cover in the Wari-Maro Protected Forest in Central Benin. https://hal.archives-ouvertes.fr/hal-02929836

[20] Solly, A. (2021) Land Use Challenges, Sustainability and the Spatial Planning Balancing Act: Insights from Sweden and Switzerland. *European Planning Studies*, **29**, 637-653. https://doi.org/10.1080/09654313.2020.1765992

[21] El Garouani, A. and Aharik, K. (2021) Apport des images landsat à l'étude de l'évolution de l'occupation du sol dans la plaine de saïss au maroc, pour la période 1987-2018. *Revue Française de Photogrammétrie et de Télédétection*, **223**, 173-188. https://doi.org/10.52638/rfpt.2021.490

[22] Bergeri, R. and Michel, J.-P. (2002) Boutin: Everything-or Almost Everything-You Need to Know About the Kappa Coefficient. *Médecine Tropicale*, **62**, 634-636. https://www.researchgate.net/publication/237658832_POUR_TOUT_SAVOIR_OU_PRESQUE_SUR_LE_COEFFICIENT_KAPPA

[23] Yemelong Temgoua, N. and Mengue, Y.W. (2022) Quantifying the Dynamics of Agricultural Land Use in the City of Yaoundé (Cameroon). *Mutations Spatiales et Sociétales Africaines*, **1**, 124-149. https://hal.science/hal-03795107

[24] Bogaert, J., Ceulemans, R. and Salvador-Van Eysenrode, D. (2004) Decision Tree Algorithm for Detection of Spatial Processes in Landscape Transformation. *Environmental Management*, **33**, 62-73. https://doi.org/10.1007/s00267-003-0027-0

[25] Barima, Y.S.S., Barbier, N., Bamba, I., Traoré, D., Lejoly, J. and Bogaert, J. (2009) Dynamique paysagère en milieu de transition forêts-savane ivoirienne. *Bois & Forets des Tropiques*, **299**, 15-25. https://doi.org/10.19182/bft2009.299.a20419

[26] N'Guessan, Y.J., Kablan, K.R., Ouattara, N.D., Douffi, K.G.-C., Gnahoré, É. and Koné, M. (2022) Anthropogenic Impact and Land-Use Dynamics in the Sangoué Protected Forest in Central-Western Côte d'Ivoire. *Afrique Science*, **21**, 8-91. https://www.researchgate.net/publication/367645936_Impact_des_Intrusions_Paysannes_sur_la_Physionomie_et_la_Dynamique_de_la_Vegetation_de_la_Foret_Classee_de_Laouda_au_Centre-Ouest_de_la_Cote_d'Ivoire

[27] Bamba, I., Mama, A., Neuba, D., Koffi, K., Traore, D., Visser, M., *et al.* (2008) Influence des actions anthropiques sur la dynamique spatio-temporelle de l\'occupation du sol dans la province du Bas-Congo (R.D. Congo). *Sciences & Nature*, **5**, 49-60. https://doi.org/10.4314/scinat.v5i1.42151

[28] Dan Tani Abdourahamane, A., Manzo Ousmane, L., Moussa Abdoul Aziz, M. and Moussa Ibrahim, D. (2025) Dynamiquespatio-temporelle de loccupation du sol de la foret classee de kouroungoussaou au Niger. *International Journal of Advanced Research*,

13, 884-899. https://doi.org/10.21474/ijar01/22170

[29] Kountangni, M.G., Yabi, I. and Toko Imorou, I. (2019) Mapping Environmental Dynamics along the Natural Grazing Routes of Cattle Herds in the Municipality of Savalou, Benin. *Revue Scientifique et Technique Forêt et Environnement du Bassin du Congo*, **12**. 35-47. http://doi.org/10.5281/zenodo.2610516

[30] Toyi, M.S., Barima, Y.S.S., Mama, A., André, M., Bastin, J.F., De Cannière, C., Sinsin, B., *et al.* (2013) Tree Plantation Will Not Compensate Natural Woody Vegetation Cover Loss in the Atlantic Department of Southern Benin. *Tropicultura*, **31**, 62-70.

[31] Agbanou, B.T., Orekan, A.O.V., Abdoulaye, D., Paegelow, M. and Tente, B. (2018) Dynamique spatio-temporelle de l'occupation du sol en zone d'agriculture extensive: cas du secteur natitingou-boukoumbe au nord-ouest du benin. https://univ-tlse2.hal.science/hal-02092545v1

[32] Tsozué, D., Basga, S.D. and Nzeukou, A.N. (2020) Spatial Variation of Soil Weathering Processes in the Tropical High Reliefs of Cameroon (Central Africa). *Eurasian Journal of Soil Science* (*EJSS*), **9**, 92-104. https://doi.org/10.18393/ejss.659830

[33] Bahri, E.M., Haboudane, D., Bannari, A., Bonn, F. and Chillasse, L. (2017) An Attempt to Map Dominant Forest Species in the Middle Atlas (Morocco) Using ASTER Data. *Teledetection*, **7**, 283-301. https://hal.science/hal-01946833v1

[34] Vischel, T., Lebel, T., Panthou, G., Quantin, G., Rossi, A. and Martinet, M. (2017) The Return of a Wet Period to the Sahel? Marseille. IRD Éditions, 43-60. https://books.openedition.org/irdeditions/12322?lang=en

[35] Descroix, L., Diongue Niang, A., Panthou, G., Bodian, A., Sane, Y., Dacosta, H., *et al.* (2015) Évolution récente de la pluviométrie en afrique de l'ouest à travers deux régions: La sénégambie et le bassin du Niger Moyen. *Climatologie*, **12**, 25-43. https://doi.org/10.4267/climatologie.1105

[36] Nouaceur, Z. (2020) The Return of Rainfall and the Resurgence of Flooding in the Sahelian Region of West Africa. *Physio-Géo*, **15**, 89-109. http://journals.openedition.org/physio-geo/10966

[37] Chagnaud, G. (2022) Changes in the Rainfall Regime in the West African Sahel: Detection, Attribution Factors, and Projections. These de Doctorat d' Université Grenoble Alpes.

[38] Siradji, A.A., Maarouhi, I.M., Mahamane, M., Ousseini, A.G., Latif, H.N.A., Soumana, D., *et al.* (2024) Dynamique spatio-temporelle des écosystèmes de la réserve de biosphère de gadabédji dans la zone nord sahélienne au centre du Niger. *European Scientific Journal*, *ESJ*, **20**, Article 310. https://doi.org/10.19044/esj.2024.v20n18p310

[39] RECA (2012) Traitement du bassin versant et du kori1 de Youri/Quels enseignements 5 ans après la réalisation des aménagements. https://reca-niger.org/spip.php?article513

[40] Ali, A., Hamadou, W.A., Ganda, R., Douma, S., Inoussa, M.M., Mahamane, A. and Saadou, M. (2023) Palmeraie de l'Aïr: Services écosystémiques et dynamiques des populations. *IOSR Journal of Pharmacy and Biological Sciences*, **18**, 1-14.

[41] Kanembou, L. (2006) Study of the Dynamics of Pastoral Areas in the Department of Gouré: Contributions of Remote Sensing and GIS. Niger-Master's Degree in Geography, University of Niamey.

[42] Cissé, F.B. (2019) Étude des impacts de l'exploitation artisanale de l'or en République de Guinée (cas de la préfecture de Siguiri). Mémoire de maîtrise en Sciences de l'environnement, Université du Québec à Montréal, 176 p. https://archipel.uqam.ca/12475/1/M15934.pdf

[43] Adamou, H.W. (2021) Ecology and Socioeconomic Importance of Phoenix dactylifera L. in the Agadez Region. Master's 2 in Ecological Science and Sustainable Biodiversity Management.

[44] Patrick, Y.A. (2024) Impact des activités d'orpaillage sur les environnements hydrologiques et la recharge des aquifères: Cas du département de Dimbokro (Centre est de la côte d'ivoire). Sciences de l'environnement, Université félix-houphouët boigny de dimbokro. https://theses.hal.science/tel-05509760/

[45] Doamba, M.U. (2024) Quatre essais sur l'exploitation minière, la forêt et le bien-être dans les pays en développement. Economies et finances. Thèse de Doctorat d' Université Clermont. https://theses.hal.science/tel-05372449

Appendix

Table A1. Landscape status.

Classes	Superficie en ha			
	2000	2005	2015	2025
Affleurement rocheux	1111080.957	512953.662	1227189.941	1423175.977
Cordon ripicole	291801.526	857032.227	1175626.172	1131983.887
Steppe	1467161.572	1742429.297	326986.206	288335.913
Erg du Ténéré	4740986.719	4473082.031	4835419.141	4777148.047
Guelta/Mare	30516.891	56048.938	76282.434	20864.825